Final Report for AFOSR

(Contract Number: AOARD-05-4077)

Research Title: Investigation of Anion Effects in Ionic Liquid-Nano Hybrid Materials

Research Institute: Korea Institute of Science and Technology

Principal Investigator: Dr. Eun Joo Roh

- Department: Medicinal Chemistry Research Center
- E-mail address : r8636@kist.re.kr
- Mailing address : P.O.Box 130-650, Cheongryang, Seoul, Korea
- Phone : +82-2-958-6779
- Fax : +82-2-958-5189

Co-Investigator:

- Dr. Jae Kyun Lee: Principal Technical Scientist, Medicinal Chemistry Research Center at KIST
- Ms. Min Jung Park: Research Scientist, Medicinal Chemistry Research Center
- Mr. Jung Hwan Park: Ph.D. Student, Sogang University
- Dr. Bang Sook Lee: Post.doc
- Ms. Eunjung Lee : Research Scientist, Medicinal Chemistry Research Center

Date: June 23, 2006

Project Leader: Eun Joo Roh

to **US Air Force Office of Scientific Research**

Report Documentation Page

Form Approved
OMB No. 0704-0188

1. REPORT DATE	2. REPORT TYPE	3. DATES COVERED
15 SEP 2006	**Final Report (Technical)**	**19-08-2005 to 23-06-2006**

4. TITLE AND SUBTITLE	5a. CONTRACT NUMBER
Investigation of Anion Effects in Ionic Liquid-Nano Hybrid Materials	**FA520905P0627**
	5b. GRANT NUMBER
	5c. PROGRAM ELEMENT NUMBER
6. AUTHOR(S) **Eun Joo Roh**	5d. PROJECT NUMBER
	5e. TASK NUMBER
	5f. WORK UNIT NUMBER
7. PERFORMING ORGANIZATION NAME(S) AND ADDRESS(ES) **Korea Institute of Science and Technology,39-1 Hawolgok-dong, Seongbuk-gu,Seoul 136-791,KOREA,KE,136-791**	8. PERFORMING ORGANIZATION REPORT NUMBER
9. SPONSORING/MONITORING AGENCY NAME(S) AND ADDRESS(ES) **The US Resarch Labolatory, AOARD/AFOSR, Unit 45002, APO, AP, 96337-5002**	10. SPONSOR/MONITOR'S ACRONYM(S) **AOARD/AFOSR**
	11. SPONSOR/MONITOR'S REPORT NUMBER(S) **AOARD-054077**

12. DISTRIBUTION/AVAILABILITY STATEMENT
Approved for public release; distribution unlimited

13. SUPPLEMENTARY NOTES

14. ABSTRACT
The project investigated the following research areas: 1) Investigation of anion effects on the hydrohpilicity/hydrophobicity using self-assembled monolayers (SAMs) of thiol-functionalized ionic liquids on gold surfaces, 2) Construction of chips that resist nonspecific adsorption of proteins using thiol-functionalized ionic liquids, 3) Generation of stimuli-responsive redox-switchable surface on gold electrodes, and 4) Hybridization of ionic liquids with CNTs and investigation of anion effects on the solubility of the IL-CNT hybrid materials.

15. SUBJECT TERMS
Carbon nano tubes, Ionic liquids, nanomaterials

16. SECURITY CLASSIFICATION OF:			17. LIMITATION OF ABSTRACT	18. NUMBER OF PAGES	19a. NAME OF RESPONSIBLE PERSON
a. REPORT	b. ABSTRACT	c. THIS PAGE			
unclassified	**unclassified**	**unclassified**		**13**	

1. Objectives

The aim of this project is investigation of anion effects on the hydrohpilicity/hydrophobicity, electron transfer using self-assembled monolayers (SAMs) of ionic liquids and on the solubility of the ionic liquid-canrbon nanotube (IL-CNT) hybrid materials toward development of novel bio-sensing, redox-switchable and conducting materials.

The specific aims are as follow:

Specific Aim 1. Investigation of anion effects on the hydrohpilicity/hydrophobicity using self-assembled monolayers (SAMs) of thiol-functionalized ionic liquids on gold surfaces

Specific Aim 2. Construction of chips that resist nonspecific adsorption of proteins using thiol-functionalized ionic liquids

Specific Aim 3. Generation of stimuli-responsive redox-switchable surface on gold electrodes

Specific Aim 4. Hybridization of ionic liquids with CNTs and investigation of anion effects on the solubility of the IL-CNT hybrid materials

2. Summary of Results

Specific aim 1: Various thiol-functionalized ionic liquids bearing oxygen-containing *N*-substituents have been synthesized starting from commercial readily available imidazole. The effects of anion on hydrophilicity/hydrophobicity of the self-assembled monolayers of the thiol-functionalized ionic liquids coated on gold surfaces were investigated by measuring water-contact angles using contact angle goniometry.

Specific aim 2: Chips coated with SAMs presenting imidazolium salt on the gold have been prepared for the surface plasmon resonance (SPR) spectroscopy (Biocore 2000), and investigated the non-specific binding of a protein, lysozyme.

Specific aim 3: To elucidate the difference in stimuli response between imidazolium salt and imidazole, the surface coated with imidazole on gold electrodes, SAMs of thiol-functionalized imidazole on gold electrode have been formed, and investigated the effects of pH on electron transfer.

Specific aim 4: Imidazolium cation-based ionic liquid has been incorporated into the multi-walled carbon nanotubes via covalent bond. The structure and anion exchange for all of modified CNTs were clearly confirmed by various analytical tools such as IR, Raman, XPS, TEM, and TGA. UV-vis analysis also performed to elucidate the effects of anion on the solubility in water and chloroform. It was also found that the ionic liquid-CNT hybrid materials showed preferential solubility in ionic liquids.

3. Publications and Awards

1. “pH-Dependent Rectification in Self-Assembled Monolayers Based on Electrostatic Interaction” *Chem. Commun..* **2006**, 183.
2. “Functionalized imidazolium salts for task-specific ionic liquids and novel materials” Chem. Commun. (Feature article), **2006**, 1049.
3. “Covalent modification of Multi-walled Carbon Nanotubes with Imidazolium-based Ionic

Liquids" **2006**, 18, 1546.

4. Chang Sea Hee Academic Awards from Korean Chemical Society, Oct. 21, **2005**.

4. Accomplishments

4-1. Synthesis of thiol-functionalized ionic liquids and formation of SAMs on gold surfaces to investigate the effects of anion on surface hydrphilicity/hydrophobicity and non-specific adsorption of proteins

All new thiol-functionalized ionic liquids were synthesized by reaction of the 12-bromo-1-thioacetyldodecane with the corresponding N-substituted imidazoles, followed by hydrolysis of thioacetyl group and anion exchange. SAMs (**1a**-**1d**, **2**-**7**) presenting imidazolium salt formed on the gold chip (Figure 1) provided by Biacore for the surface plasmon resonance (SPR) spectroscopy (Biocore 2000) upon soaking them in solutions of the appropriate thiol for 24 h.

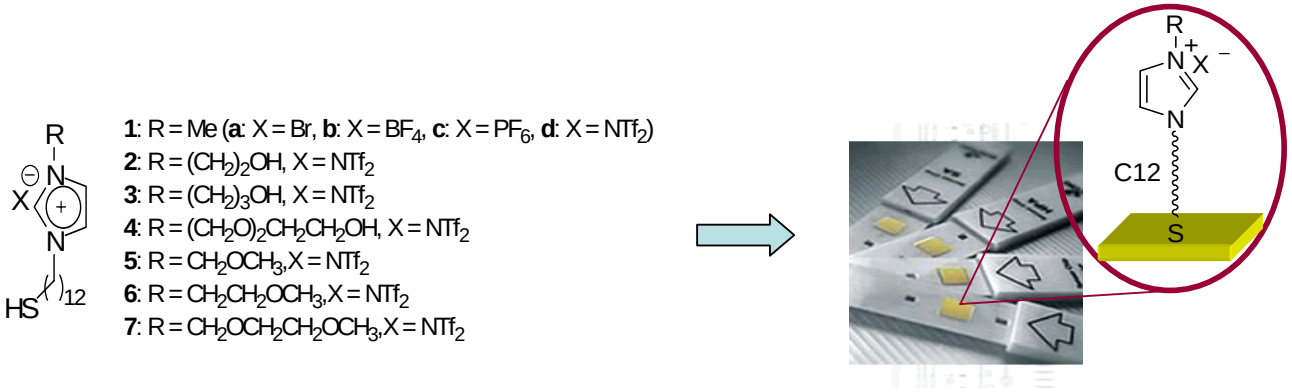

Figure 1. Synthesized thiol-functionalized ionic liquids and formation of SAMs on gold chip, which used for surface plasmon resonance spectroscopy (SPR) study

Our previous electrochemical study on SAM **1a** clearly indicated that thiol-functionalized imidazolium salts formed a well-ordered, closed-packed monolayer on gold. Based on the electrochemical study results and the thickness measured by ellipsometry suggest that the all of the SAMs used in this study formed a monolayer. To investigate the effect of counter anion on lysozyme adsorption, the SAMs **1a**-**1d** presenting 1-methylimidazolium salts having different counteranions chose as model SAMs since the effects of N-substituents on protein adsorption could be minimized. As we demonstrated previously, the water wettability of the SAMs largely dependent on the counter anion, thus, the SAMs **1a**,**b** bearing Br and BF_4 anions are hydrophilic whereas the SAM **1c** having PF_6 counter anion is relatively hydrophobic, and the most hydrophobic SAM is **1d** showing the highest water contact angle (65°).

Table 1. Thiol-functionalized ionic liquids and their thickness and water contact angles of the SAMs on gold surfaces

SAMs	thickness (Å)	contact angle (°)
1a	19	23
1b	-	35
1c	-	52
1d	-	65
2	21	22
3	23	25
4	26	35
5	23	65
6	22	68
7	24	70

For adsorption of lysozyme to SAMs **1a**-**1d**, the lysozymes were dissolved in phosphate buffer (1 mg/mL) at pH 7.4. The surface was exposed to protein solution for 120 second, and rinsed with PBS for 120 second. The amount of adsorbed protein is proportional to the difference between the reflective units (RU) obtained from the SPR sensograms after and before exposure to protein solution ($\Delta RU = RU_{\text{after exposure}} - RU_{\text{before exposure}}$). Figure 2 shows the sensorgrams of the adsorption of lysozyme to SAMs of 1a-1d. Interest finding is that the adsorption of lysozyme to the SAMs was largely affected by the counteranion, however, not much by the wettability of the surfaces affected dominantly by anion. The SAM **1a** and SAM **1d** having the most hydrophilic Br and hydrophobic NTf_2 counter anions, respectively, showed the higher resistance toward the nonspecific adsorption of the protein. We do not understand the origin of these anion effects and have not studied them in detail to speculate. Nevertheless, these results clearly indicate that the counteranion of imidazolium salts could play an important role in their interactions with biomolecules.

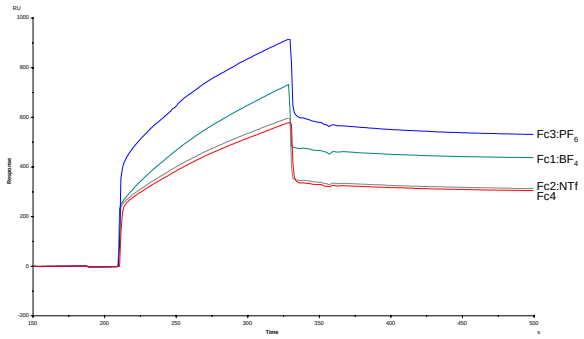

Figure 2. Plots of ΔRU as a function of time for the adsorption of lysozyme to SAMs **1a**-**1d**. The curves were adjusted vertically to have the same value of ΔRU at the time when the lysozyme began to flow over the SAM. The region of time during which protein was present in the buffer is indicated above the plot. The buffer conditions for these experiments were as follow: 10 mM sodium phosphate, 2 mM potassium phosphate, 137 mM NaCl, 2.7 mM KCl, pH 7.4. Proteins were dissolved in buffer at 1 mg/mL.

We next investigated the effects of N-substituents in imidazolium cation on the adsorption of lysozyme to SAMs **2**-**7** and the counteranion was fixed with the effective NTf_2. For comparison, we also studied the protein adsorption to the surface of a CM5 sensor chip (Biacore), which is a gold surface coated with partially carboxymethylated dextran, and typically used as the background in SPR experiments. For convenient comparison of the protein resistance ability of the ionic liquid SAMs with the CM5, relative amount of adsorbed lysozyme (%ML) was calculated from ΔRU values taken from sensorgrams according to the following equation: $\%ML = \Delta RU_{IL} \times 100/\Delta RU_{CM5}$, which summarized in figure 3.

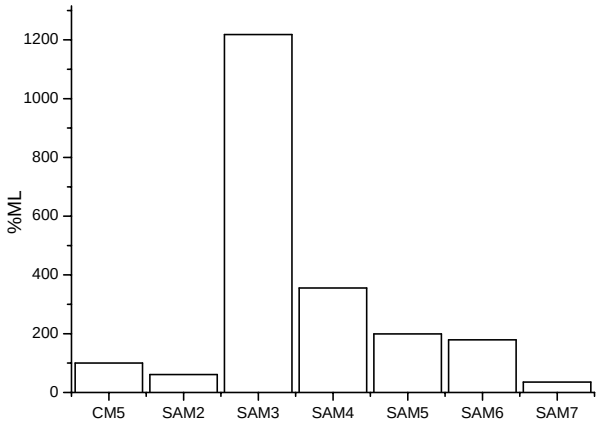

Figure 3. Relative amount of adsorbed lysozyme (%ML) was calculated from ΔRU values taken from sensorgrams according to the following equation: $\%ML = \Delta RU_{IL} \times 100/\Delta RU_{CM5}$

A comparative protein-adsorption experiment showed that the SAM **2** (%ML = 61) presenting hydroxyethylimidazolium is significantly more protein resistant than commercially available dextran-based sensor chip CM5 surface. However, when the length of the alkyl chain was elongated one-carbon forming SAM **3** (%ML = 1218), the ability of protein resistant was dramatically decreased. The SAM **4** bearing $(CH_2O)_2CH_2CH_2OH$ group also showed relatively poor protein resistance (%ML = 355). With respect to the criteria formulated by Whiteside and co-workers regarding the molecular structure of protein-resistant materials, it is not surprising that the more hydrophilic SAM **2** show the better protein-resistant property than the relatively hydrophobic SAMs **3** and **4**. However, much of the previous work has suggested that the SAMs terminating polyoxygenated alcohols would be more hydrophilic than the SAMs terminating simple alkyl alcohols, and thus, would be more protein adsorption resistant surface. Therefore, the results from water wettability and protein adsorption could imply that the imidazolium moiety of the SAMs may cooperatively effect on the surface wettability as well as protein adsorption. However, the hydrophilicity of a surface alone is not a sufficient feature to effectuate protein resistance. The sensorgrams obtained from the OH free SAMs **5**-**7** showed that the better protein resistance was observe with relatively more hydrophobic SAM **7** (%ML = 35) terminating $CH_2OCH_2CH_2OCH_3$ group than the hydrophilic SAMs **5** (%ML = 199), **6** (%ML = 179) and even than the dextran-based CM5. This observation is in good agreement with the hypothesis referring to the absence of hydrogen-bond donors, and could be ascribed to the higher flexibility and dynamics of the terminal $CH_2OCH_2CH_2OCH_3$ group in SAM **7** compared with those of the $CH_2CH_2OCH_3$ and CH_2OCH_3 terminal groups in SAMs **5** and **6**.

4-2. Generation of stimuli-responsive redox-switchable surface on gold electrodes

In preliminary study, we accomplished the anion-directed $Ru^{+3/+2}$ redox-switch on gold electrode. To elucidate the difference in stimuli response between imidazolium salt and imidazole, the surface coated with imidazole on gold electrodes was investigated. The effects of pH on the electron transfer kinetics of ferrocenemethanol (FcOH)/$FcOH^+$ redox couple, *i.e.* pH dependent rectification, was investigated for the first time. In (FcOH)/$FcOH^+$ redox couple, it was found that the direction of electron transfer could be dependent on pH. When the imidazole group is deprotonated form, access of both FcOH and $FcOH^+$ to the electrode was allowed for bidirectional electron transfer (**Figure 4a**). The protonated imidazole group at low pH, however, the positively charged $FcOH^+$ will be repulsed and will not be exerted any force on the neutral FcOH. These asymmetric electrostatic interactions may influence the electron transfer kinetics of oxidation and reduction asymmetrically. At this pH, therefore, unidirectional electron transfer was observed (**Figure 4b**).

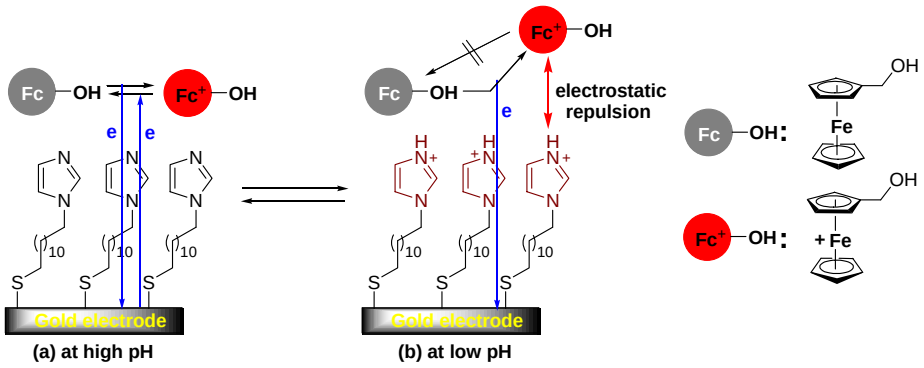

Figure 4. Schematic presentation of pH dependent rectification

Cyclic voltammetry was used to confirm whether the SAM enables the electrochemical rectification. A gold electrode was modified by immersion in 1-(12-mercaptododecyl)imidazole solution overnight. The potential scan was applied to this modified electrode in the acidic solution containing 0.5 mM FcOH and 10 mM KBr (pH=2) until steady cyclic voltammogram (CV) was obtained. Although the electron transfer through the monolayer to FcOH was hindered at the first scan, oxidation current was increased during repeated potential scans. After 5-7 cycles of the potential scan, a steady CV, demonstrating unidirectional electron transfer, was obtained. After the steady CV was acquired, pH of the solution was altered repeatedly between 2 and 12 on the same electrode. The typical characteristic CV of electrochemical rectifier, normal oxidation current and suppressed reduction current, was observed at pH 2 while the usual CV of bidirectional electron transfer was obtained at pH 12 (Figure 5a). There are three important features in Figure 5: first, no voltammetric feature corresponding to the reduction of $FcOH^+$ is observed at pH 2, suggesting that the protonated imidazole effectively prevented the penetration of the positively charged $FcOH^+$. On the other hand, the peak current of the oxidation, as high as that on the naked bare gold electrode, exhibits the facile oxidation of FcOH. Therefore, unidirectional electron transfer is clear from the CV at pH 2. Second, the peak potential in anodic current is near the oxidation potential of FcOH on the naked bare gold electrode. In previously reported electrochemical rectifications using mediated electron transfer, the peak potential is determined by the redox potential of mediating molecule. In contrast, the peak potential of electrochemical rectifier based on electrostatic repulsion depends on the redox potential of solution-phase electroactive probe molecule. Third, the reversible switching between unidirectional and bidirectional electron transfer is possible (Figure 5b). This switching shows that the resulting structure of the SAM induced by potential sweeps is stable during further potential scans and the alternation of pH. All these results demonstrate the pH-dependent electrochemical rectification due to the asymmetric electrostatic interaction.

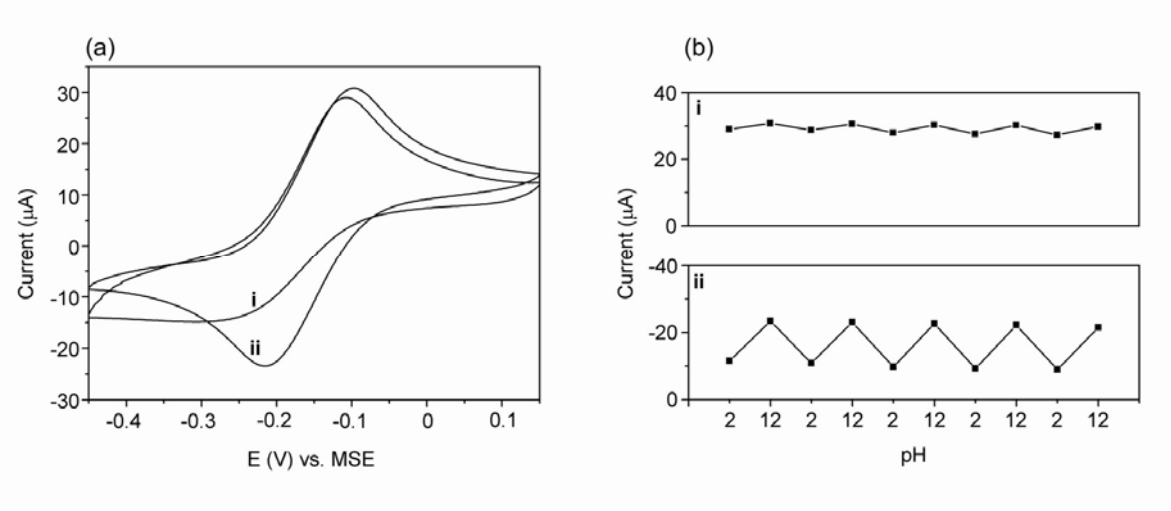

Figure 5. (a) CVs on the SAM-modified Au in a solution containing 0.5 mM ferrocenemethanol and 10 mM KBr (i) at pH = 2 and (ii) at pH = 10. Facile oxidation of FcOH and suppressed reduction of $FcOH^+$ is observed at pH 2. CV at pH 12 demonstrates the characteristic features of bidirectional electron transfer. Scan rate = 50 mV/s. (b) Variation in (i) the anodic peak current and (ii) the cathodic peak current during the repeated alternation of pHs.

4-3. Hybridization of ionic liquids with multi-walled carbon nanotubes, and investigation of anion effects on solubility

Methods for the functionalization of MWCNTs with imidazoluim salts are depicted in Scheme 1. The chemical oxidation of pristine MWCNTs were carried out in a 60% aqueous HNO_3 under sonication condition to yield carboxylic acid-functionalized MWCNTs, ***f*-1**.

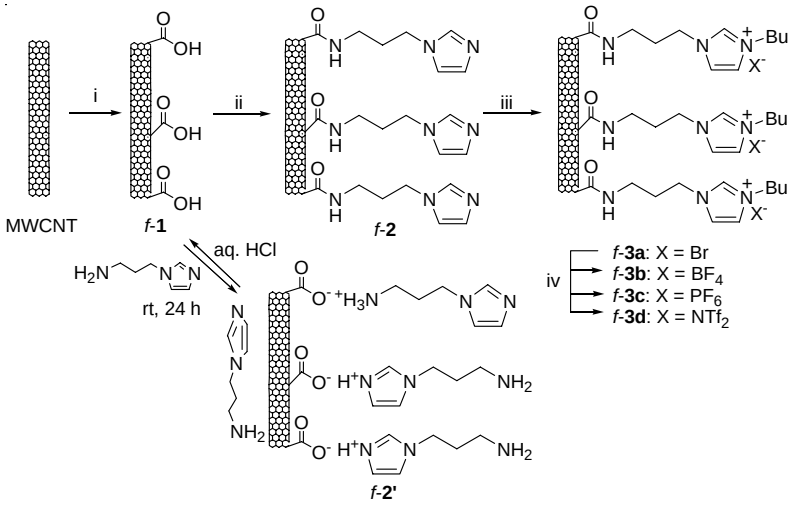

Scheme 1. (i) 60% aqueous HNO_3, sonication for 1.5 h, 50 ^oC. (ii) a) $SOCl_2$, reflux, 24 h; b) 3-aminopropylimidazole, 120 ^oC, 24 h. (iii) (***f*-3a**): *n*-BuBr, 80^oC, 24 h. (iv) for ***f*-3b**: ***f*-3a** + $NaBF_4$ in H_2O, 24 h; for ***f*-3c**: ***f*-3a** + $NaPF_6$ in H_2O, 24 h; for ***f*-3d**: ***f*-3a** + $LiNTf_2$ in H_2O, 24 h.

In Raman spectra (Figure 6a), increased R value (intensity of D_a/G_a) of the ***f*-1** (R = 1.4) was observed compared with the pristine MWCNTs (R = 1.3) suggesting that the defect of CNTs was increased during functionalization. The presence of carboxylic acid groups was clearly confirmed by IR analysis, in which the C=O bands appeared at 1718 and 1568 cm^{-1} with about 1:1 intensity (Figure 6b). The carboxylic acid group of ***f*-1** was converted to acid chloride, which was subsequently reacted with an excess amount of 3-aminopropylimidazole at 120 ^{o}C for 24 h under nitrogen atmosphere. The resulting MWCNTs were washed thoroughly successively with THF and 1N aqueous HCl solution to remove the excess 3-aminopropylimidazole and any non-covalently adsorbed substances. Finally, the substrates were washed with deionized water and ethanol, and dried to afford 3-aminopropylimidazole-functionalized MWCNTs (***f*-2**). In the IR spectrum of ***f*-2**, the C=O band of the carboxylic acid group at 1718 cm^{-1} in ***f*-1** was shifted to 1646 cm^{-1}, indicating the formation of the amide bond. The qualitative X-ray photoelectron spectroscopy (XPS) analysis of ***f*-2** also showed the nitrogen atom (N1s, 401 eV) (Figure 7a) suggesting the presence of imidazole moiety in ***f*-2**. In order to confirm the covalent bond formation in ***f*-2**, the control experiments were also carried out with the aminopropylimidazole salt ***f*-2'**, which was prepared independently by mixing ***f*-1** and 3-aminopropylimidazole at room temperature for 24 h. Both the substrates, ***f*-2** and ***f*-2'**, were treated with 1 N aqueous HCl solution at room temperature, and the resulting substrates were subjected to the XPS analysis.

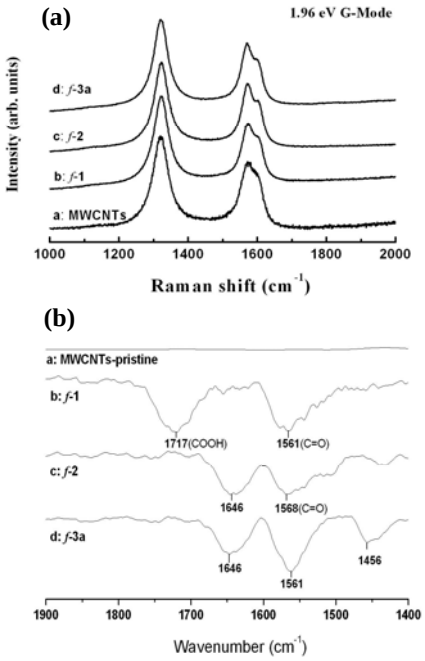

Figure 6. (a) D and G bands of the Raman spectra for a: pristine MWCNTs (area ratio of D_a/G_a, R = 1.30), b:***f*-1** (R = 1.40), c:***f*-2** (R = 1.35), and d: ***f*-3a** (R = 1.38). (b) C=O bands of FT-IR spectra of a: pristine MWCNTs, b: ***f*-1**, c: ***f*-2**, d: ***f*-3a**.

As shown in Figure 2, the nitrogen peaks were retained from ***f*-2** (Figure 7a) whereas they disappeared from ***f*-2'** (Figure 7b), where ***f*-2'** was converted to the carboxylic acid-functionalized MWCNT, ***f*-*1***. These results clearly indicate that the aminopropylimidazole moiety in ***f*-2** was covalently bonded onto the surface of MWCNTs and the non-covalently adsorbed 3-aminopropylimidazole moieties onto the surface of MWCNTs could be removed by washing with aqueous HCl solution. The quantity of the aminopropylimidazole in ***f*-2** was determined from the thermogravimetric analysis (TGA) of ***f*-2**, which showed a 11.7 weight% loss corresponding to the aminopropylimidazole fragments, and from this value the mole % of the aminopropylimidazole moiety on the surface of MWCNTs ($[AI]_{MWCNT}$ = 1.13 mol % with respect to carbon) was calculated by using the weight% and the molecular weight of the aminoimidazole fragment (124.16 $gmol^{-1}$). The *N*-butylimidazolium bromide-functionalized MWCNT (***f*-3a**) was prepared by the reaction of ***f*-2** with excess *n*-butylbromide (Scheme 1). In the ^1H NMR spectrum of ***f*-3a**, the protons of the imidazolium ring resonated at δ 8.9 and 7.5 ppm, which clearly indicated the formation of imidazolium bromide salts. The XPS analysis of ***f*-3a** further confirmed the formation of imidazolium bromide salt (Br: $3d_{3/2}$, 70 eV and $3d_{5/2}$, 69 eV) (Figure 7c). The bromide anion of ***f*-3a** could be exchanged with other anions such as BF_4 (***f*-3b**), PF_6 (***f*-3c**) and NTf_2 (***f*-3d**) by treatment with $NaBF_4$, $NaPF_6$ and $LiNTf_2$, respectively, in deionized water at room temperature for 24 h. During the anion exchange, it was observed that the homogeneous black solution became clear and the anion-exchanged MWCNTs were precipitated. The XPS analyses of ***f*-3b**, ***f*-3c** and ***f*-3d** clearly indicated that the Br anion of ***f*-3a** was completely exchanged (Figure 6c) with BF_4^- (B1s, 194 eV and F1s, 688 eV), PF_6^- (P $2p_{1/2}$, 137 eV, $2p_{3/2}$, 136 eV and F 1s, 687 eV) and NTf_2^- (N 1s, 401 eV, 399 eV; S1s 168 eV, F1s 688 eV).

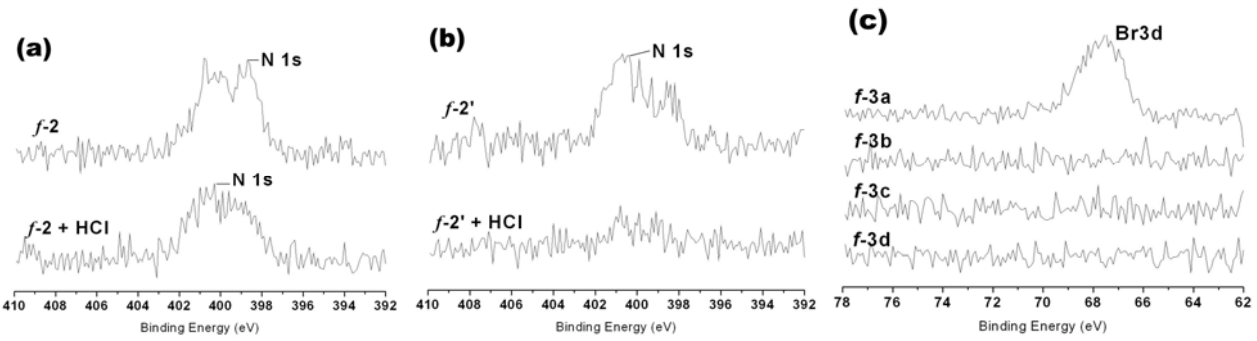

Figure 7. N(1s) region in XPS spectra of (a) ***f*-2** and (b) ***f*-2'** before (upper spectrum) and after (lower spectrum) treatment with aqueous HCl solution. (c) The Br(3d) region in XPS spectra of the ***f*-3a** and the anion-exchanged ***f*-3b**, ***f*-3c**, and ***f*-3d**.

The tubular structures of the functionalized MWCNTs were observed in the transmission electron microscopy (TEM) images, suggesting that the functionalization and anion-exchange processes did not deteriorate the structural integrity of MWCNTs (Figure 8).

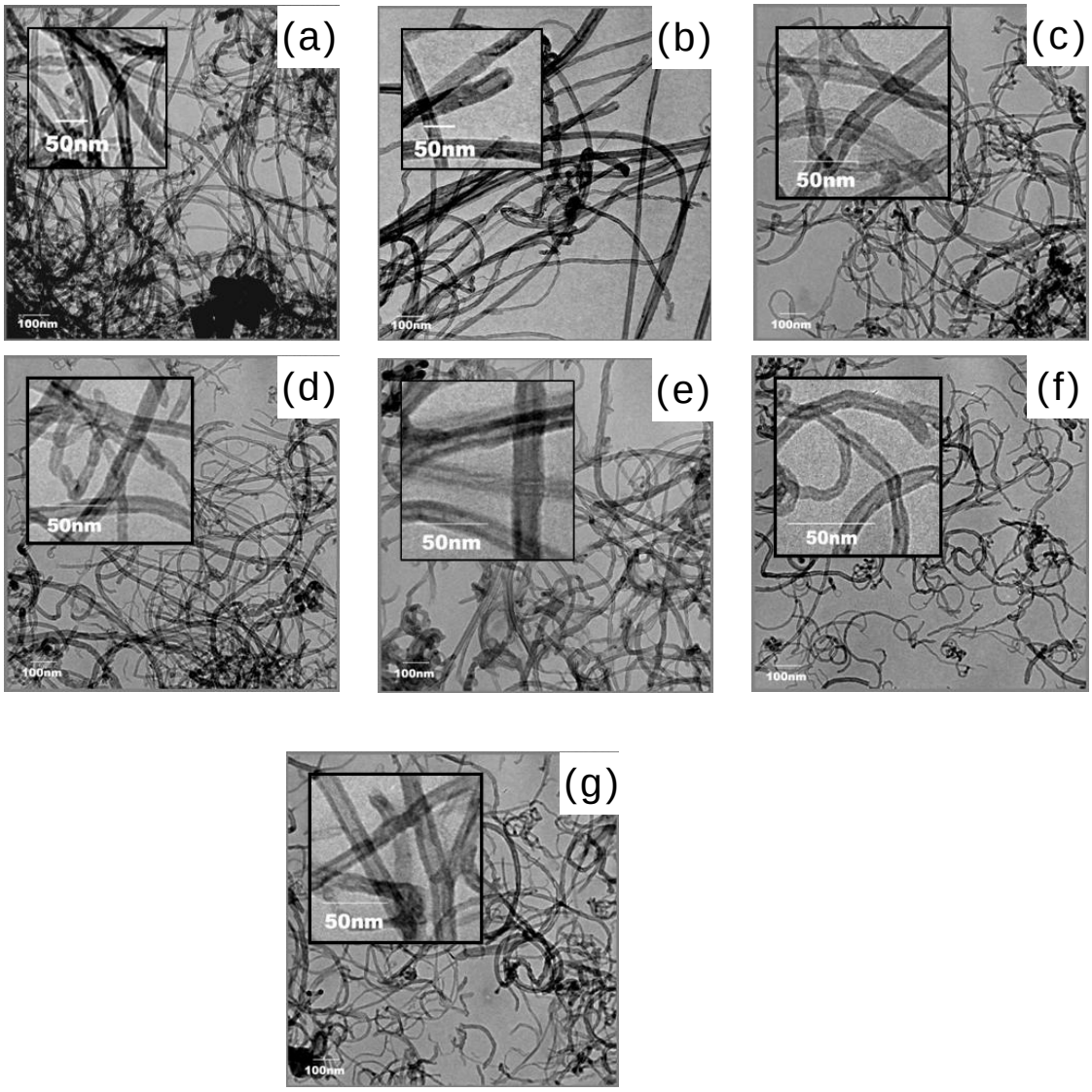

Figure 8. TEM images of the (a) pristine MWCNTs, (b) ***f*-1**, (c) ***f*-2**, (d) ***f*-3a**, (e) ***f*-3b**, (f) ***f*-3c**, and (g) ***f*-3d**.

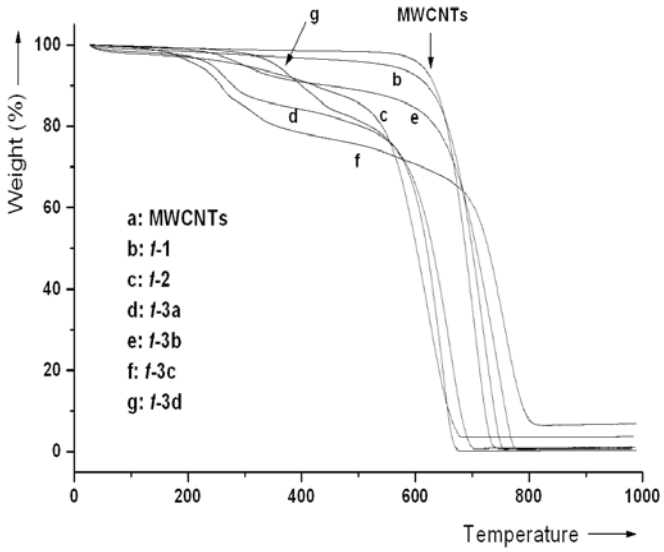

Figure 9. TGA curves (heating rate: 20^{o}C/min and air flow: 20 mL/min) of the pristine and the functionalized MWCNTs, ***f*-1**, ***f*-2**, and ***f*-3a~3d**.

The thermostability of the functionalized CNTs was investigated by using TGA (heating rate: 20^{o}C/min and air flow: 20 mL/min). As shown in Figure 9, the crude MWCNTs (Figure 9a) and ***f*-1** (Figure 9b) were thermally stable below 600^{o}C. In contrast, the aminoimidazole-functionalized ***f*-2** (Figure 9c) and the imidazoluim salt-functionalized ***f*-3a-d** (Figure 9d-g) decomposed at much lower temperature with two main weight-loss regions. The first weight-loss region below ~350^{o}C may be attributed to the decomposition of the surface-attached aminoimidazole and aminopropylimidazolium salt. The significant weight reduction in the second region (~580^{o}C) is likely due to the decomposition of MWCNTs. The comparison of the TGA curves of the imidazolium salt-functionalized MWCNTs (***f*-3a-d**) suggests that the counteranion has influence on the thermostability of MWCNTs. However, the exact nature of the effect of anions on the thermal stability of MWCNTs is not yet clear and remains to be solved.

The solubility and the dispersibility of the functionalized MWCNTs, ***f*-1, *f*-2** and ***f*-3a-d**, were semi-quantitatively characterized with a UV-Vis spectrophotometer at 600 nm in water and chloroform (Table 2). The relative absorbance of ***f*-3a-d** in water implies that the effect of counteranions on hydrophilicity/hydrophobicity of the IL-functionalized MWCNTs, *i.e.* solubility in water is the following order: ***f*-3a** (Br^-) > ***f*-3b** (BF_4^-) > ***f*-3c** (PF_6^-) > ***f*-3d** (NTf_2^-), is quite consistent with the results obtained previously from the water contact angle of the monolayered surfaces coated with 1-methylimidazolium cation.[14] The ***f*-3d** bearing NTf_2 anion, which is known to be the most hydrophobic counteranion in 1-butyl-3-methylimidazolium cation-based ionic liquids, showed the lowest absorbance in water, but the highest value in chloroform. Consistent with the UV-Vis data, ***f*-3a** with *n*-butylimidazolium bromide completely dissolved in water,

leading to the formation of homogeneous black aqueous solution. The homogeneity of ***f*-3a** in water remained after several months and no precipitation was observed.

Table 2. The absorbance at 600 nm (A_{600}) of the functionalized MWCNTs (*f*-1, *f*-2, *f*-3a~3d) with a content of 1 mg sample per 10 mL water and chloroform.

f-MWCNT / Solvent		***f*-1**	***f*-2**	***f*-3a**	***f*-3b**	***f*-3c**	***f*-3d**
H_2O	A_{600}	1.2317	1.2367	1.5784	0.3079	0.018	0.014
	R_{600}	1.000	1.004	1.281	0.250	0.015	0.011
$CHCl_3$	A_{600}	0.9375	0	1.4457	1. 2593	1. 0999	2.0419
	R_{600}	1.000	0	1.542	1.343	1.173	2.178

R is the ratio of A_{600} of the sample to A_{600} of ***f*-1**.

The imidazolium salt-functionalized MWCNTs (***f*-3a**, ***f*-3b**, ***f*-3c,** and ***f*-3d**) were quite soluble in a hydrophobic ionic liquid, [bmim][NTf_2] (bmim = 1-buthyl-3-methylimidazolium), whereas the carboxylic acid- (***f*-1**) and aminopropylimidazole-functionalized MWCNTs ***f*-2** were not soluble. Among the IL-functionalized MWCNTs, the ***f*-3d** bearing NTf_2 counteranion exhibited highest solubility in all ionic liquids. However, the other IL-functionalized MWCNTs showed preferential solubility in the ionic liquid having same counteranion with IL-functionalized MWCNTs. Thus, although the possibility of the counteranion exchange between the IL-functionalized MWCNTs and ILs when they have different counter anions could not be excluded, the ***f*-3b** and ***f*-3c** showed preferential solubility in [bmim][BF_4] and [bmim][PF_6], respectively. The anion effects on the solubility of the imidazolium salt-functionalized MWCNTs allowed the phase-transition of the MWCNT *via* direct anion exchange. Figure 9 shows the optical micrograph of the phase-transition of the functionalized MWCNTs. Upon the addition of $LiNTf_2$ (3 mg), the homogeneous black aqueous solution (1.0 mg/mL) of ***f*-3a** (Figure 4a) became colorless and precipitates were observed (Figure 10b), which could be extracted with $CHCl_3$ (Figure 10c). These results clearly indicate that the anion exchange of the Br^- with NTf_2^- changed the solvent preference of the imidazolium salt-functionalized MWCNTs between H_2O and $CHCl_3$. Moreover, the imidazolium salt-functionalized MWCNTs, even the water-soluble ***f*-3a**, exhibited a high preferential solubility in an ionic liquid, [bmim][NTf_2]. The addition of 1 mL of [bmim][NTf_2] to the aqueous solution of ***f*-3a** followed by vigorous shaking resulted in the complete transfer from the aqueous layer to the IL layer (Figure 10d). The preferential solubility of the imidazolium salt-functionalized MWCNTs

in [bmim][NTf_2] could be ascribed to strong ionic interactions between the imidazolium ions, which were covalently linked with the modified MWCNTs, and [bmim][NTf_2].

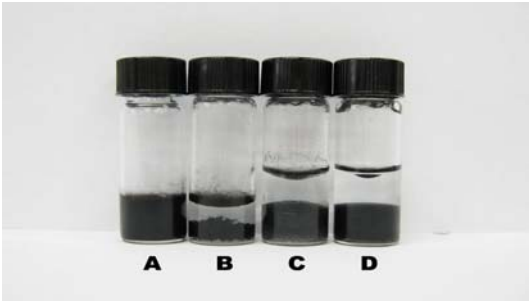

Figure 10. A photograph showing phase-transfer of the functionalized MWCNTs (1 mg/mL) via anion exchange (1 mg/mL). a: ***f*-3a** in H_2O, b: ***f*-3a** + $LiNTf_2$ in H_2O, c: extraction of b (***f*-3a** + $LiNTf_2$ in H_2O) with $CHCl_3$ (upper layer is H_2O and lower layer is $CHCl_3$, v/v = 1), and d: extraction of a (***f*-3a** in H_2O) with [bmim][NTf_2] (v/v = 1) (the upper layer is H_2O and the lower layer is [bmim][NTf_2]).